Peer-reviewed version available at *Metals* **2020**, *10*, 214; doi:10.3390/met10020214

Article

Mechanical Properties of Friction Stir Welded AA1050-H14 and AA5083-H111 Joint: Sampling Aspect

Velaphi Msomi [1,*] **and Nontle Mbana** [1]

[1] Cape Peninsula University of technology, Faculty of Engineering and the Built Environment, Mechanical Engineering Department, P.O. Box 1906, Bellville, 7535, South Africa

* Correspondence: msomiv@gmail.com; Tel.: +27 21 953 8627

Abstract: Welding of dissimilar aluminium alloys has been a challenge for a long period until the discovery of the solid state welding technique called friction stir welding (FSW). The discovery of this technique encouraged different research interests revolving around the optimization of this technique. This involves the welding parameters optimization and this optimization is categorized into two classes i.e. similar alloys and dissimilar alloys. This paper reports about the mechanical properties of the friction stir welded dissimilar AA1050-H14 and AA5083-H111 joint. The main focus is to compare the mechanical properties of specimens extracted from different locations of the welds i.e. the beginning, middle and the end of the weld. The specimen extracted at the beginning of the weld showed low tensile properties compared to specimens extracted from different locations of the weld. There was no certain trend noted through the bending results. All three specimens showed dimpled fracture which is the characterization of the ductile fracture.

Keywords: tensile strength; flexural strength; friction stir welding; microstructure; dissimilar aluminium alloys

1. Introduction

Friction stir welding (FSW) is classified as one of the welding techniques which joins materials through heat generated during friction occurring between the tool shoulder and the workpieces [1]. The invention of this welding technique was based on the materials which were classified as 'un-weldable' materials through the conventional methods. Those classified materials included certain classes of aluminium alloys. Aluminium alloys are mostly used in many industries like aviation, shipbuilding and automotive because of their lightweight. The focus towards FSW has expanded such that it includes testing the capability of the technique in welding other materials that are outside the aluminium class. This includes the welding of copper and its alloys, titanium and magnesium and its alloys [2]. When the aluminium alloys are welded with the conventional technique, they are likely to have weld splitting on the joint line. The fusion welding of aluminium alloys is difficult than the welding of steel due to their low melting point, softness, and so forth. The aluminium alloys sometimes bent and shrink when welded using conventional welding and those effects are caused by residual thermal stress [3].

FSW is known to have the best metallurgical properties when compared to fusion welding and this is caused by the microstructural modification which occurs during welding. Mishra and Ma [4] reported that to have a great weld and to avoid defect on the weld it is important to take welding parameters, material flow and heat generation into consideration during the welding process.

Peer-reviewed version available at Metals 2020, 10, 214; doi:10.3390/met10020214

There are mainly four crucial steps that are involved during the performance of FSW i.e. plunging, dwelling, welding, and pulling. The rotating tool is inserted into the butt joint slowly until the shoulder touches the surface of the workpieces (plunging). The plunged tool remains in one location for a certain period with the purpose of building up input heat (dwelling). The plunged tool moves along the plates being joined at a specified speed (welding). The rotating tool gets removed vertically from the welded plates soon after reaching the ends of the plates (pulling) and this normally leaves a hole which indicates the end of the weld [5].

There are recent studies that are being conducted with the purpose of tracking the status of FSW of aluminium alloys [6]. It has been reported that for the production of the good weld, the tool geometry and welding parameters play a very important role. This includes the rotation speed, traverse speed, tool tilt angle and plunged depth. Plunge depth has been found to be a critical parameter in the heat generation and for proper consolidation of material without defects. The plunge depth was also identified as one of the parameter which plays an important role towards the microstructural arrangement of the joint [7].

Welding dissimilar materials is quite challenging when compared with welding similar materials due to the difference in mechanical properties and chemical composition of the base materials. To acquire better weld mechanical properties, the harder material must be placed on the retreating and softer material placed in the advancing side [8-9]. The tool geometry plays a very important role in welding dissimilar materials. Welding dissimilar alloys require the use of different tool profiles such as threaded, squared and triangular profiles to transfer the material from top of the joint to bottom and vice versa by stirring movement [10]. Kundu and Singh [11] reported that tool pin profile geometry plays an important role in weld quality while the surface quality of the weld joint depends upon the tool tilt angle. The increase in tool tilt angle affects the flow and fill up of material during welding.

In most cases, the welding of dissimilar materials involves the welding of aluminium alloys which are not far from each in terms mechanical properties i.e. 5xxx will be welded together with 6xxx, 6xxx welded with 7xxx, etc. Recently, there are attempts that have been made in trying to weld the aluminium alloys that are mechanically far apart from each other i.e. FSW of AA2024 to AA6061 [12]. This investigation has used single and dual pin tool. Defect free joint were obtained in all selected parameters except the welding speed beyond 90 mm/min. The onion rings were visible on the nugget region for joints produced using dual-pin tool but absent on the single pin tool. The highest ultimate tensile strength (UTS) was obtained with the dual-pin tool at a welding speed of 150 mm/min whereas the single-pin produced the UTS at a welding speed of 90 mm/min. However, the UTS produced by single-pin was always less than the one produced by dual-pin tool.

There are various aspects that have studied through the use of dissimilar materials. This involves the analysis of the strain hardening behaviour on the friction stir welded dissimilar alloys which are mechanical far apart from each other i.e. 2024-T351 and 5083-H112, 2024-T351 and 7075-T651 [13]. This analysis was performed on two types of joints i.e. 2024-T351 and 5083-H112 with 2024-T351 on the advancing side and 5083-H112 on retreating side. The second joint was 2024-T351 and 7075-T651 with 2024-T351 on the retreating side and 7075-T651 on the advancing side. It was discovered that the strain-hardening rate of AA7075/AA2024 joint was higher than that of parent material while the strain-hardening rate of AA2024/AA5083 joint lies between those of parent material. It was also found that the tensile properties of both joints were lower than those of parent material. Xia-Wei et al. [14] did the

microstructural analysis correlatively with mechanical properties of the FSW joint using dissimilar alloys. The lamellar structure in the bottom of the nugget zone was found to be more homogeneous and finer than other regions. The hardness on the copper side of the nugget was higher than that on the aluminium side. The UTS of the joint was found to be relatively lower than that of the base metal. The tensile morphology revealed ductile-brittle fracture mode.

Kumbhar and Bhanumurthy [15] did a comparative study on friction stir welding of similar to dissimilar aluminium alloys i.e. AA5052 to AA6061 and AA6061 to AA6061. The similar and dissimilar joints were produced at various combinations of tool rotation speeds and tool traverse speeds. The microstructural analysis reveal that there was no rigorous mixing in the nugget region for both materials. The tensile properties of dissimilar material (AA5052-AA6061) were much better compared to the properties of the similar materials (AA6061-AA6061). Welding dissimilar aluminium alloys that are mechanical far apart has gained much attention and interest from researchers [16]. This includes the analysis of friction stir welding of dissimilar AA2017A-T451 and AA7075-T651 plates at a different tool rotation speed. The results reveal that the best tensile properties could be achieved when AA2017A-T451 is on the retreating side. It was also established that the material that is located on the retreating side dominates the weld centre and this is in consistent with the results reported by other researchers [8,9,13]. Ranjith and Kumar [17] analysed the impact of joining two dissimilar aluminium alloys AA2014 T651 and AA6063 T651 by friction stir welding. They discovered that the tensile strength is better when the tool is offset towards AA2014 (advancing side). When it is offset towards AA6063 (retreating side), it results in insufficient heat generation on the advancing side which then results in an incomplete fusion of AA2014. Sarsılmaz and Caydas [18] conducted a study on statistical analysis on mechanical properties of friction-stir-welded AA1050-H14/AA5083-H321 couples. The study investigated the effect of friction stir welding parameter focusing on rotational speed, traverse speed, and stirrer geometry. On their investigation, they discovered that traverse speed has significant effect on UTS and nugget hardness. Their analysis also included the optimized welding parameters to be used in welding the said aluminium alloys.

The analysis of the effect of material positioning during FSW has gone outside the aluminium family. This includes the study which analysed the effect of location variation in FSW of steel with different carbon content. It was discovered that the placement of stronger material on the advancing side reduces the weld nugget size and increases the amount of martensite formation. The location of the strongest material on the advancing side lead to higher temperature and stress due to the highest temperature on the advancing side [19]. It is evident from the literature that the FSW that involves materials that are mechanically apart involves mainly 2xxx as the weaker material. There are very few studies which utilized AA1xxx [18].

This paper reports on the mechanical properties of the weld produced by friction stir welding technique using AA1050-H14 and AA5083-H111. The analysis is performed on the specimens extracted in different locations of the weld. This type of analysis will give an information regarding the best location for sampling the welds produced from the materials with extreme unique properties.

2. Experimental procedure

The 6mm thick AA1050 and AA5083 plates were cut into 70mm X 530mm long using a guillotine cutting machine (see fig. 1).

Peer-reviewed version available at Metals 2020, 10, 214; doi:10.3390/met10020214

Figure 1. Aluminium alloy plates

The two dissimilar plates were fixed on the back plate of the FSW machine as shown in fig. 2. The AA5083-H111 was kept on the retreating side throughout the experiments while AA1050-H14 was on the advancing side. This kind of material location was followed based on the recommendation from the literature [8,9,13,16,25,26]. The plates were fixed on the machine back plate by eight clamps. The function of clamps was to make sure the plates do not move apart when the rotating pin is in motion.

Figure 2. FSW machine

The plates were then friction stir welded using high carbon steel (H13) tool shown in fig. 3. The tool was machined using lathe machine and was heat treated to about 50HRB. The profile of the pin was triangular threaded with 20mm shoulder diameter and 6mm pin diameter. The triangular threaded pin had 1mm pitch and the height of 5.8mm. The FSW parameters used in this study are presented in Table 1 and these parameters were chosen based on various speed tests combinations performed prior to the main welding. However, those trail results are not included in this work since they are not part of the paper's focus.

Table 1. FSW parameters.

Rotational speed (rpm)	Traverse speed (mm/min)	Tilt angle (^{0})
1000	30	2

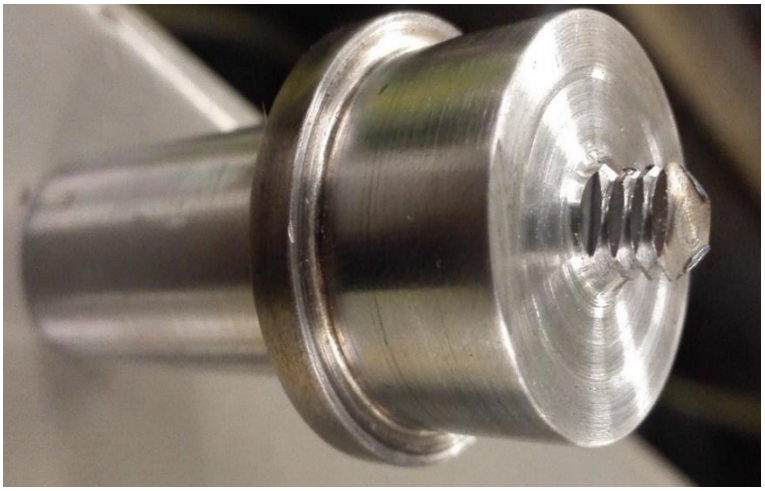

Figure 3. FSW tool

Fig. 4 shows the friction stir welding of 6 mm thick AA1050 and AA5083 plates. Stage 1 shows two plates ready for welding. Stage 2 shows the rotating tool plunged into the two pieces being welded i.e. AA1050 and AA5083. Stage 3 shows the welded part of the plates. Stage 4 shows the end of FSW and the unplunging of the tool. The finished product is clearly shown in fig.5. The chemical composition for materials used in this study is presented in Table 2.

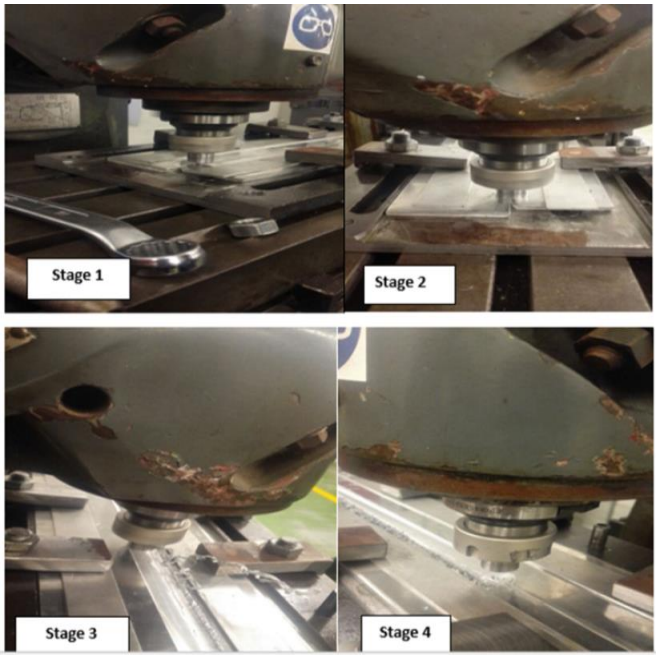

Figure 4. Friction stir welding process.

Preprints (www.preprints.org) | NOT PEER-REVIEWED | Posted: 12 December 2019 doi:10.20944/preprints201912.0156.v1

Peer-reviewed version available at Metals 2020, 10, 214; doi:10.3390/met10020214

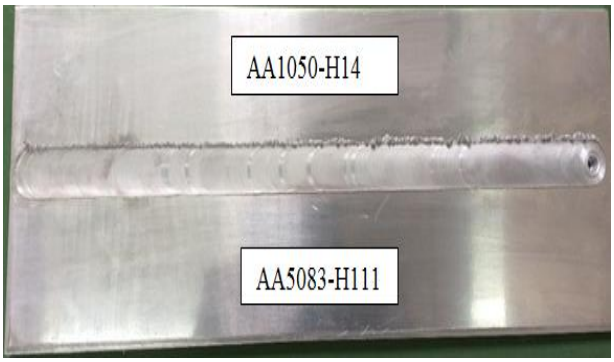

Figure 5. FSW joint.

Table 2. Chemical composition of AA1050 and AA5083 [wt%]

Material	Si	Fe	Cu	Mn	Mg	Cr	Zn	Ti	Al
AA1050-H14	0.10	0.29	0.01	-	0.02	-	0.01	0.02	Balance
AA5083-T111	0.14	0.20	0.01	0.65	4.62	0.10	0.01	0.01	Balance

3. Welded joint analysis

This section describes the mechanical and microstructural analysis of the welded joint. This includes the use of tensile test machine, microstructure analysis, bending test and scanning electron microscope (SEM). It should be noted that the friction stir welded joint had a start, middle and ending points. The specimens were all labelled A, B, and C. Label A indicates the specimens cut at the beginning of the joint, specimens cut in the middle were labelled B while C symbolize the specimens cut at the end of the joint. This format was followed throughout the performance of the tests.

3.1. Tensile test

The machine that was used for the tensile test was the Hounsfield tensometer (universal testing machine). The tensile test specimens were cut perpendicular to the welding direction (see fig. 6). The tensile test specimens were designed according to the ASTM E8M-04 standard [24] for accurate dimensions. The specimens were cut using CNC wire cutter and the coordinates for cutting specimens were manually generated using 2D drawings in Solidworks shown in fig. 7. This method of cutting was selected because it does not induce heat during cutting.

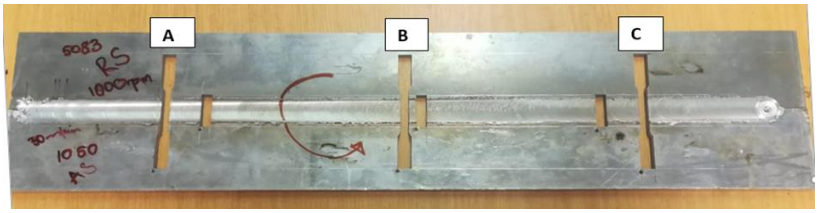

Figure 6. FSW plate showing specimen positioning.

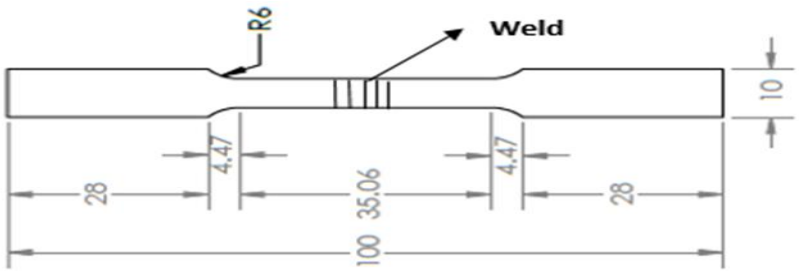

Figure 7. Tensile test specimen.

The tensile test parameters used in this study are presented in Table 3. The specimens were tensile tested until they fracture (see fig. 10).

Table 3. Tensile test parameters.

Speed (mm/min)	Extension range (mm)	Load range (kN)
3	0-10	0-10

3.2. Microstructure Analysis

The microstructure analysis was performed using the Nikon Eclipse L150 microscope. The microstructure was observed under polarized slider with an Axiocam 105 colour camera for acquiring the pictures. The specimens were cut into 26x8x6mm using the CNC wire cutter and prepared for analysis using Keller's reagent etchant.

3.3. Bending Test

Three-point bending tests were conducted using the same Hounsfield tensometer previously used for the tensile tests. The machine parameters used were similar to those used for tensile tests. There were six rectangular shape specimens prepared for bending tests. The bending tests were performed on the face and the root of the joint. The three specimens presented in fig. 8 show the face of the joint (the surface that was in contact with the tool shoulder) and another three presented in fig. 9 show the root of the joint (the surface that was in contact with the back-plate). For comparative purposed, bending test was also performed on parent materials.

Figure 8. Bending specimens (face).

Peer-reviewed version available at *Metals* **2020**, *10*, 214; doi:10.3390/met10020214

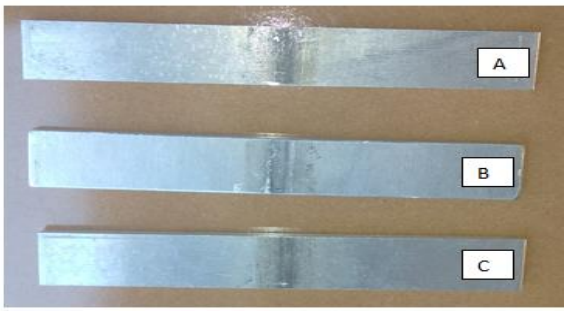

Figure 9. Bending specimens (root).

3.4. Scanning Electron Microscope (SEM)

The SEM used was the Zeiss Auriga. Prior to the analysis, the samples were coated with a layer of carbon to ensure sufficient conductivity during analysis. The results obtained are presented and explained in the next section.

4. Results and discussion

The detailed discussions of the results obtained from the various test performed are presented in this section. The results obtained includes the tensile test, bending test, microstructure and SEM analysis**.**

4.1. Tensile test

Figure 10 shows the fractured specimens post tensile tests. It was observed that the fracture occurred on the advancing side (AA1050) of the specimen. This behaviour suggests that the weld joint is mechanically stronger than the AA1050 alloy [8,9,25]. This also suggests that the welded joint was dominated by AA5083-H111 hence it was stronger [13,26].

Figure 10. Fractured specimens.

Table 4 shows the results of the ultimate tensile stress (UTS) and percentage elongation. The AA1050 and AA5083 show the UTS of 104.89MPa and 326.75MPa respectively, while the FSW specimens A, B and C show 50.67MPa, 66.47MPa and 63.19MPa respectively. The UTS for the joint was lower than that of the parent materials. This suggests that the joint elongates quicker compared to parent materials. The percentage elongation was found to be 19%, 25% and 26% for specimen A, B and C respectively. These indicate that the FSW specimens' B and C were more ductile compared to the specimen A and AA1050 parent material but less ductile compared to parent material AA5083.

Peer-reviewed version available at Metals 2020, 10, 214; doi:10.3390/met10020214

Table 4. Tensile test results.

Specimen	Ultimate Tensile strength (UTS) (MPa)	Percentage elongation
A	50.67	19%
B	66.47	25%
C	63.19	26%
1050 Parent	104.89	23.5%
5083 Parent	326.75	33.5%

Figure 11 shows the tensile test-strain curve of AA1050, AA5083 and FSW specimens A, B and C. The UTS of the parent material AA5083 is larger than that of the parent material AA1050 and of the FSW specimens. Specimen A which is the first specimen from the welded plate is the weakest while specimen B and C are close to each other. This behavior is assumed to be caused by insufficient heat input at the beginning of the weld. The temperature stabilizes from the middle to the end of the plate hence improved UTS.

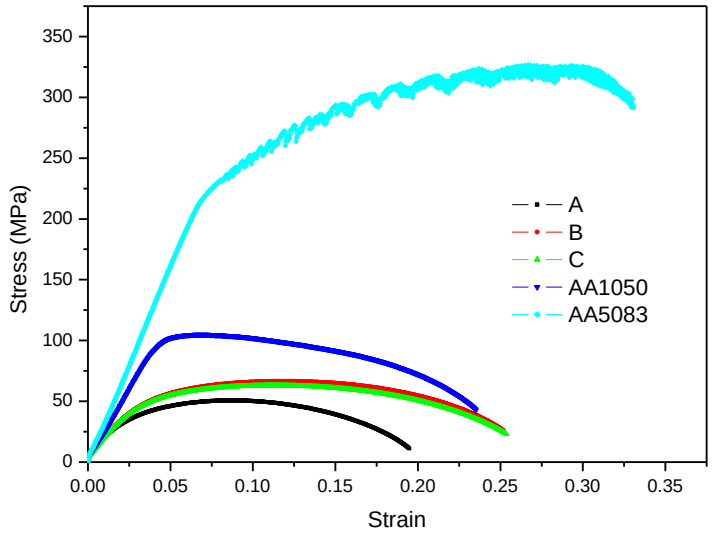

Figure 11. Stress-strain curve

4.2. Bending Test

Figures 12 and 13 are the post- bending test specimens for FSW and parent materials. The reddish-brown line appearing on specimens in fig. 12 (a) and (b) indicates the center of the joint. The face and the root bending occurred towards the advancing side of the joint. This behavior suggests that the joint was mechanically stronger compared to AA1050 hence bending occurred on the advancing side. This behavior is in agreement with the behavior observed in the tensile analysis. The post-bending results showed the tested specimens without failure. This means that the welded materials have bonded well during welding.

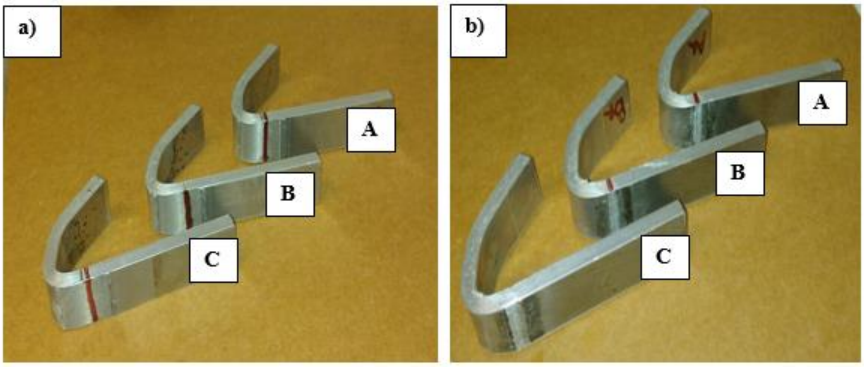

Figure 12. a) Tested bending specimen (face), b) Tested bending specimen (root)

Figure 13. Tested bending specimen (parent material)

Figures 14 and 15 shows bending stress and strain curves of the joint together with parent materials. As it has been mentioned before that all the welded specimens bent on AA1050, the flexural stresses for both face and root are within the range of that of AA1050 (see Table 5). The average stress for face and root is 218.94MPa and 259MPa, respectively. These values suggest that the root side of the weld is stronger than that of the face. This could be caused by the fact that the lower side of the weld was exposed to the restricted downward movement due to bed backing plate. The flexural stress values are comparatively higher than the tensile values and this is due to higher temperatures involved during FSW.

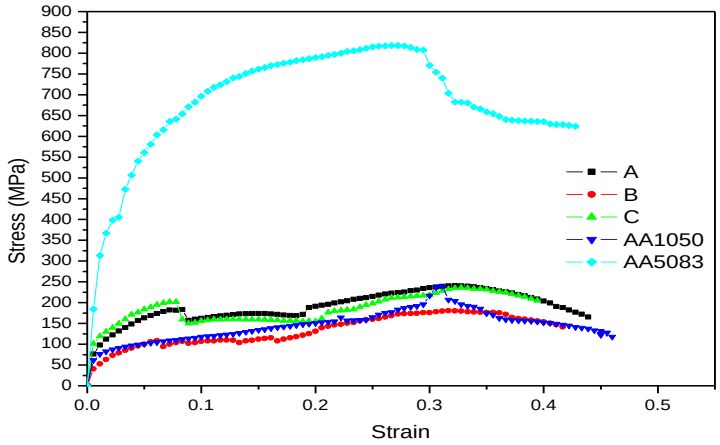

Figure 14. Bending stress – strain curves (face).

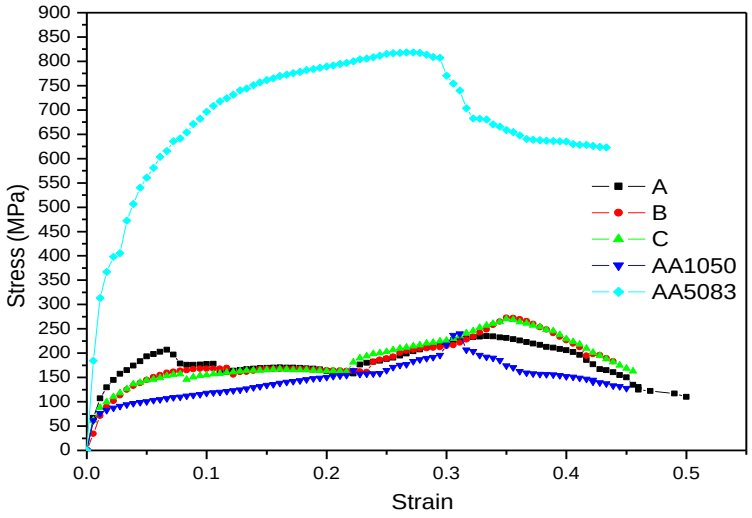

Figure 15. Bending stress – strain curves (root).

Table 5. Bending test results.

Specimen	Flexural strength (MPa)	Flexural strain
Face		
A	240.56	0.43
B	180.38	0.41
C	235.88	0.39
Average stress	218.94	
Root		
A	234.75	0.5
B	272.25	0.44
C	270	0.45
Average stress	259	
Parent Materials		
AA1050	240.19	0.46
AA5083	818.44	0.44

4.3. Microstructure

The FSW joint is characterized by four different zones as shown in fig. 16. Those zones include weld nugget (WN) around the weld center line, thermo-mechanically affected zone (TMAZ) on both sides of the weld nugget/stir zone, heat affected zone (HAZ) which is surrounding the TMAZ, and non-affected base metal (BM) of AA1050 and AA5083 [9-15]. The regions originate from the material flow behaviour caused by the tool rotation. Figures 18-20 show the microstructural grains for the base metals and the welded region. Figure 17 shows the microstructural grains for AA1050 base metal. The measured grain size for the base metal AA1050 was in the range of 25 - 33μm while the grain size for AA5083 base metal (shown in figure 18) ranged between 6.6 - 8μm. The microstructural arrangement of the stir zone is shown in figure 19. The

measured grain size for the stir zone or welded region ranged between 7.3-11.4 μm. The grain size range for the stir zone is close to the grain size range for AA5083 base metal. The morphology for the stir zone is similar to that of AA5083 base metal with some visible elongated whitish traces in between. These whitish elongated traces are assumed to be the residual trace of AA1050 which was pulled towards AA5083 side during welding.

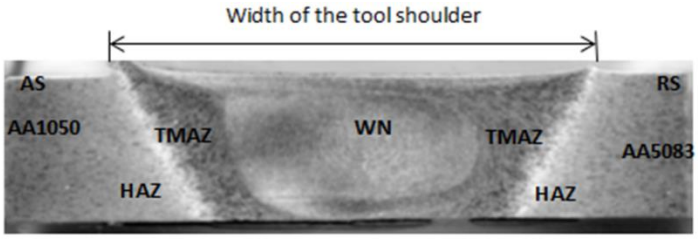

Figure 16. Macrostructure of the welded join as WN- weld nugget, TMAZ: thermo-mechanical affected zone, HAZ: heat affected zone.

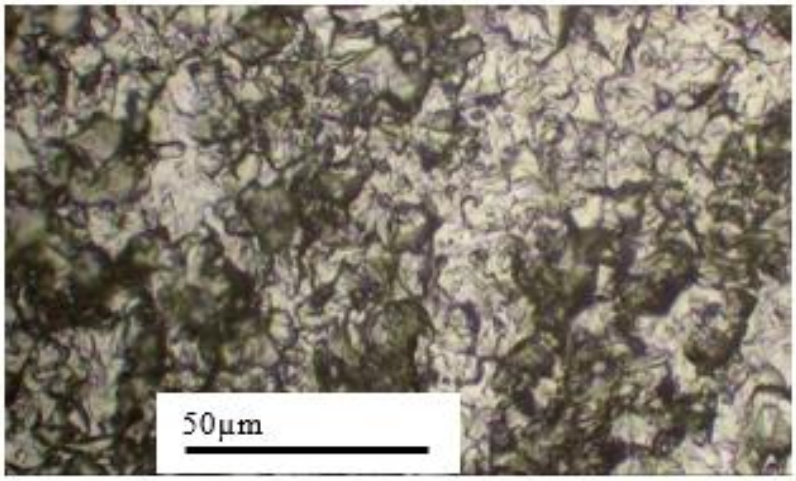

Figure 17. Micrograph for 1050 base metal

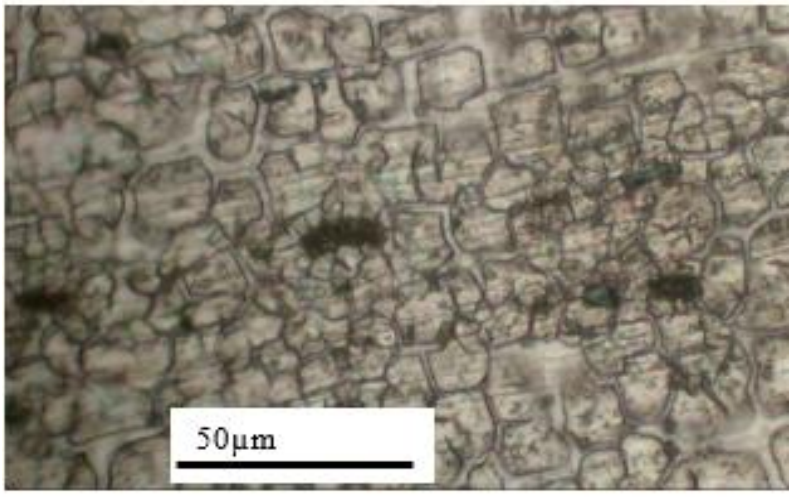

Figure 18. AA5083 base metal

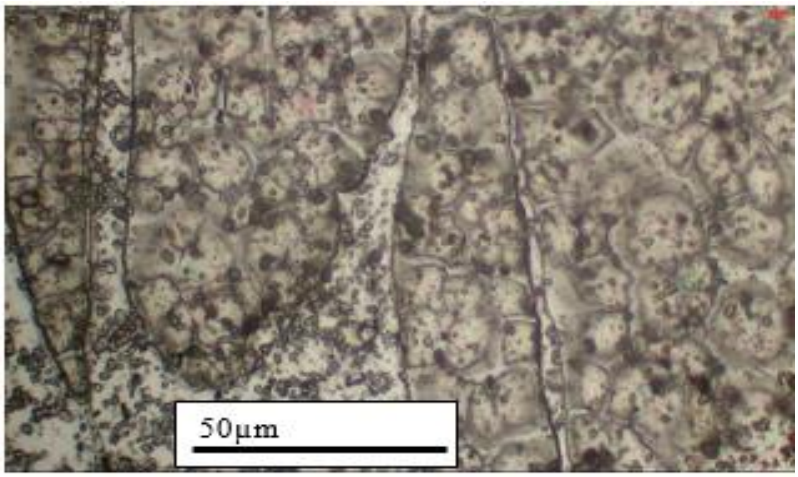

Figure 19. Micrograph for stir zone

4.4. Scanning Electron Microscopy (SEM)

It should be noted that the fractured surface for base metals were studied comparatively with specimen C. The elimination of other specimens was due to the fact that there was no distinction on the surface morphology for the other specimens. All the specimens show a cup like dimpled fracture which is a characterization of ductile failure mode [25]. The similarity in surface fracture suggests that the ductility of the materials involved in the joint formation was preserved post welding even though there are some percentage elongation variations.

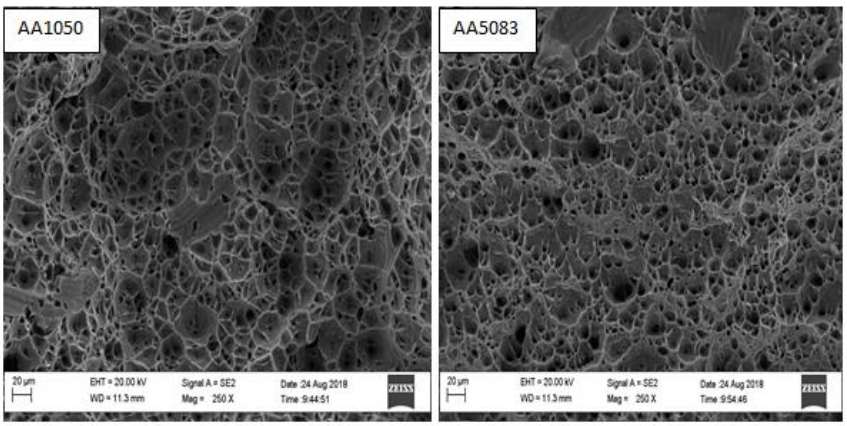

Figure 20. Micrograph of parent material**.**

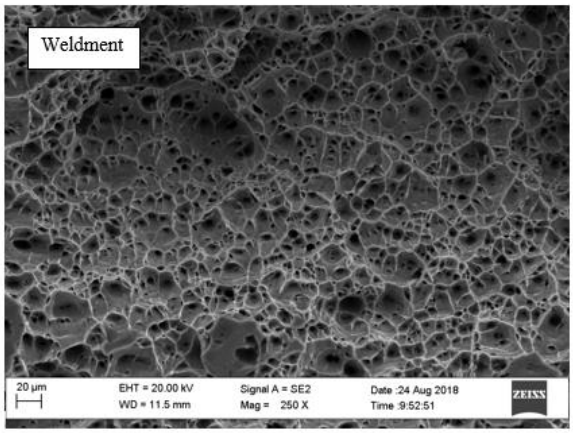

Figure 21. Micrograph of the welded specimen.

5. Conclusions

In summary, the welding of AA1050-H14 and AA5083-H111 was found to be feasible through the use of the mentioned welding parameters. The UTS for the joint was found to be lower than the UTS for parent materials. In addition to this, the specimen extracted at the beginning of the weld exhibited lowest UTS compared to the specimens extracted from other locations of the weld. The ductility of the joint was fluctuating between the that of the parent materials. The fracture location was found to be consistent with the one reported in the literature [8,9,13]. The grain size of the joint was found to be in the range of the stronger parent material (AA5083-H111) and there were no notable differences from the three specimens. The morphology of the fracture surface indicated ductile failure mode which was characterized by cup-like dimples for all the specimens.

Author Contributions: Authors have contributed equally to this work.

Funding: This research received no external funding.

Acknowledgments: Authors would like to thank Mr EM Masekwana for his technical assistance during welding.

Conflicts of Interest: The authors declare no conflict of interest.

References

1. Mishra, R.S.; and Mahoney, W. Friction stir welding and processing. *ASM International*, **2007**, 368.
2. Thomas, W.; and Nicholas, E. Friction stir welding for the transportation industries. *Mat. Des.*, 18(4–6), **1997**, 269–273.
3. Genevois, C.; Deschamps, A.; Denquin, A.; and Boisneau-Cottignies, B. Quantitative investigation of precipitation and mechanical behaviour for AA2024 friction stir welds. *Act. Mat.*, 53(8), **2005,** 2447–2458.
4. Mishra, R.S.; and Ma, Z.Y. Friction stir welding and processing. *Mat. Sc. Eng.*, 50, **2005**, 1–78.
5. Farias, A.; Batalha, G.F.; Prados, E.F.; and Magnabosco, R. Tool wear evaluations in friction stir processing of commercial titanium Ti-6Al-4V. *Int. J. Sc.Techn. Fric. Lub. Wr.*, 302, **2013**, 1327–1333.
6. Tiwari, S.K.; Shukla, D.K.; and Chandra, R. Friction Stir Welding of Aluminium Alloys: A review. *Int. J. Mech. Aer. Ind. Mechat. Manuf. Eng.*, 7(12), **2013**, 1326–1331.

7. Soundarajan, V.; and Yarrapareddy, E. Investigation of the friction stir lap welding of aluminium alloys AA 5182 and AA 6022. *J. Mat. Eng. Perf.*, 16(4), **2007**, 477–484.

8. Sadeesh, P.; Rajkumar, P.; Avinash, N.; Arivazhagan, K.; and Narayanan, S. Studies on friction stir welding of AA 2024 and AA 6061 dissimilar metals. *Proc. Eng.*, 75, **2014**, 145–149.

9. Amancio-Filho, S.T.; Sheikhi, S.; dos Santos, J.F.; and Bolfarini, C. Preliminary study on the microstructure and mechanical properties of dissimilar friction stir welds in aircraft aluminium alloys 2024-T351 and 6056-T4. *J. Mat. Proc. Techn.*, 206, **2008**, 132–142.

10. Biswas P.; and Kumar, D.A. Friction stir welding of aluminium alloy with varying tool geometry and process parameters. *J. Eng. Man.*, 226, **2011**, 641.

11. Kundu, J.; and Singh, H. Friction stir welding of dissimilar Al alloys : Effect of process parameters on mechanical properties Friction stir welding of dissimilar Al alloys. *Eng. Sol. Mech.*, 4, **2016**, 125-132

12. Hou, W.; Shen, Y.; Huang, G.; Yan,Y.; Guo, C.; and Li, J. Dissimilar friction stir welding of aluminium alloys adopting a novel dual-pin tool: Microstructure evolution and mechanical properties. *J. Man. Proc.*, 36, **2018**, 613–620.

13. Niu, P.L.; Li, W.Y.; and Chen, D.L. Strain hardening behaviour and mechanisms of friction stir welded dissimilar joints of aluminium alloys. *Mat. Let.*, 231, **2018**, 68–71.

14. Xia-wei, L.I.; Da-tong, Z.; Cheng, Q.I.U.; and Wen, Z. Microstructure and mechanical properties of dissimilar pure copper / 1350 aluminium alloy butt joints by friction stir welding. *Trans.Nonf. Met. Soc. China*, 22(6), **2012**, 1298–1306.

15. Kumbhar, N.T.; and Bhanumurthy, K. Friction Stir Welding of Al 5052 with Al 6061 Alloys. *J. Met.*, 2012, **2012**, 7-10

16. Kopyściański, M.; Węglowska, A.; Pietras, A.; Hamilton, C.; and Dymek, S. Friction Stir Welding of Dissimilar Aluminium Alloys. *K. Eng. Mat.*, 682, **2016**, 31-37.

17. Ranjith, R.; and Senthil Kumar, B. Joining of dissimilar aluminium alloys AA2014 T651 and AA6063 T651 by friction stir welding process. *W. Trans. App. Theo. Mech.*, 9, **2014**, 179–186.

18. Sarsılmaz, F and Çaydaş, U. Statistical analysis on mechanical properties of friction-stir-welded AA 1050/AA 5083 couples. *Int. J. Adv. Man. Techn.*, 43(3–4), **2009**, 248–25

19. Choi, D. H.; Lee, C. Y.; Ahn, B.W.; Yeon, Y. M.; Park, S.H.C.; Sato, Y. S.; Kokawa, H.; and Jung, S. B. Effect of fixed location variation in friction stir welding of steels with different carbon contents. *Sc. Techn. Weld. Join.*, 15, **2010**, 299–304.

20. Koilraj, M.; Sundareswaran, V.;Vijayan, S.; and Koteswara Rao, S.R.. Fricriction stir welding of dissimilar aluminium alloys AA2219 to AA5083 - Optimisation of process parameters using Taguchi technique. Mat. Des., 42,**2012**, 1-7.

21. Patel, V.; Li, W.;Wang, G.;Wang, F.; Vairis, A.; Niu, P. Friction Stir Welding of Dissimilar Aluminum Alloy Combinations: State-of-the-Art. Met. **2019**, 9, 270.

22. Jesusa , J.S.; Gruppelaara, M.; Costaa, J.M.; Loureiroa, A.; and Ferreira, J.A.M. Effect of geometrical parameters on Friction Stir Welding of AA 5083-H111 T-joint. *Proc. Str. Int.*, 1, **2016**, 242–248.

23. Sato, Y., Urata, M., Kokawa, H., Ikeda, K. Hall–Petch relationship in friction stir welds of equal channel angular-pressed aluminium alloys, *Mat. Sc. Eng*. 354 (1–2), **2003**, 298–305.

24. Annual Book of ASTM Standards. Standard Test Methods for Tension Testing of Metallic Materials, *ASTM International, 01*, **2004**.

25. MD S., Birru, AK. Mechanical and metallurgical properties of friction stir welded dissimilar joints of AZ91 magnesium alloy and AA 6082-T6 aluminium alloy. *J. Magn. All.* 7, **2019**, 264–271.

26. Azeez, S., Mashinini, M., Akinlabi, E. Sustainability of friction stir welded AA6082 plates through post-weld solution heat treatment. *Proc. Manuf.*,33, **2019**, 27-34.